Physica D 238 (2009) 1000–1007

Contents lists available at ScienceDirect

Physica D

journal homepage: www.elsevier.com/locate/physd

Modeling cardiac mechano-electrical feedback using reaction-diffusion-mechanics systems

R.H. Keldermann [a,*], M.P. Nash [b], A.V. Panfilov [a]

[a] Department of Theoretical Biology, Utrecht University, Padualaan 8, Utrecht, 3584 CH, The Netherlands

[b] Auckland Bioengineering Institute and Department of Engineering Science, The University of Auckland, New Zealand

ARTICLE INFO

Article history:
Available online 3 September 2008

Keywords:
Reaction-diffusion systems
Mechanics
Stretch activated channels
Mechano-electrical feedback
Spiral wave breakup

ABSTRACT

In many practically important cases, wave propagation described by the reaction-diffusion equation initiates deformation of the medium. Mathematically, such processes are described by coupled reaction-diffusion-mechanics (RDM) systems. RDM systems were recently used to study the effects of deformation on wave propagation in cardiac tissue, so called mechano-electrical feedback (MEF). In this article, we review the results of some of these studies, in particular those relating to the effects of deformation on pacemaker activity and spiral wave dynamics in the heart. We also provide brief descriptions of the numerical methods used, and the underlying cardiac physiology.

1. Introduction

Reaction-diffusion (RD) equations describe a wide variety of non-linear systems in physics, chemistry and biology. They describe non-linear wave patterns in the Belousov–Zhabotinsky (BZ) chemical reaction [1], in the processes of morphogenesis of the mould *Dictyostelium discoideum* (Dd) [2], of electrical activity in cardiac tissue [3], and in many other biological systems. More information about reaction-diffusion systems can be found in [4,5]. Propagation of non-linear waves is usually accompanied by other important processes. One of the most fundamental is the mechanical deformation of the medium. In the human heart, non-linear electrical waves propagate through the cardiac tissue and initiate cardiac contraction. In turn, mechanical deformation also affects the electrical waves of the heart. This sets up a complex system of feedback between both of these processes, and is known as mechano-electrical feedback (MEF) [6–8]. In this article, we review modeling approaches used to study MEF using coupled reaction-diffusion-mechanics systems. We start with a description of the physiological basis of cardiac excitation, contraction and MEF. We then outline the modeling approach and its numerical implementation, and present results on the effects of MEF on the initiation of ectopic beats, pacemaking activity, and spiral wave dynamics in the heart. We limit our studies to wave dynamics in two dimensions. Review articles discussing other aspects of MEF can be found in [9–11].

Biophysics of cardiac excitation and contraction. Cardiac contraction is initiated by the propagation of electrical waves. The waves are a result of timed excitation of billions of cardiac cells (myocytes), which are electrically coupled together via conducting gap junctions.

Electrical activation of a cardiac cell is a sudden change of its transmembrane potential, from the resting state (around −90 mV), to an excited state (around +10 mV). This change of transmembrane potential occurs as a result of several transmembrane currents carried by various ions (Na^+, K^+, Ca^{2+}, Cl^-, etc.) across the cell membrane. These currents can be subdivided into two large groups: inward currents, which depolarize (excite) cardiac cells, and outward currents, which repolarize the membrane to its resting state. The inward currents are carried mainly by Na^+ and Ca^{2+} ions, and the outward current are mainly carried by K^+ ions. Excitation of the cell occurs if the transmembrane potential exceeds the threshold value (approximately −60 mV). After that the inward Na^+ current is activated and brings the membrane potential to its fully activated state of around 10 mV. After depolarization, a repolarization phase follows, in which the membrane potential slowly recovers to its resting membrane potential due to inactivation of Na^+ current and activation of the outward K^+ currents. The time-course of excitation of a cardiac cell and the main inward (negative) and outward (positive) currents involved are schematically shown in Fig. 1.

If a cell becomes excited (depolarized), current from this cell propagates to neighboring cells via the gap junctions, which in turn cause neighboring cells to depolarize. As soon as the threshold value of the transmembrane potential is reached, these cells also become excited and in a similar way transmit excitation to their neighbors. This results in a propagating wave of excitation.

* Corresponding author.
E-mail addresses: r.h.keldermann@bio.uu.nl (R.H. Keldermann), A.Panfilov@uu.nl (A.V. Panfilov).

0167-2789/$ – see front matter © 2008 Elsevier B.V. All rights reserved.
doi:10.1016/j.physd.2008.08.017

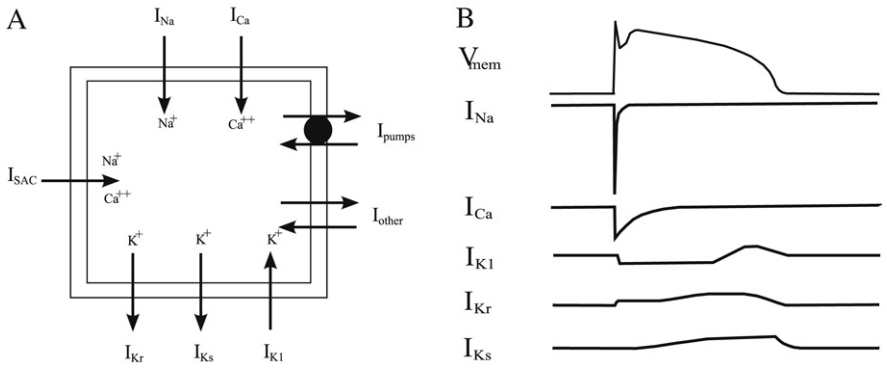

Fig. 1. (A) Schematic overview of inward and outward ion currents across the surface cell membrane. (B) Schematic time plot of currents during the action potential phase.

Excitation of the heart initiates cardiac contraction in the following way. During depolarization, a small amount of calcium ions flows into the cell through the calcium channels. This calcium current causes a subsequent release of a larger quantity of calcium stored within specialized cellular compartments called the sacroplasmatic reticulum. This increases the calcium concentration initiates contraction of the heart via calcium mediated conformational changes in contractile proteins (troponin-C, actin, myosin) [8]. Initiation of contraction via excitation is called electro-mechanical (or excitation–contraction) coupling.

There is also a feedback effect of contraction on excitation of cardiac cells, which is known as mechano-electrical feedback. The main physiological mechanism underpinning this is believed to be mechano-sensitive ion channels, such as the stretch activated channels (SAC), which have been identified in cardiac cells [12,13]. In response to cell stretch, these channels produce an inward current [8] which as we discussed above, tends to depolarize the cell and in some cases can even initiate cardiac excitation. Franz et al. [14] showed that mechanical stimulation of the heart induced by periodic expansion of a balloon placed into the heart ventricle results in the induction of electrical excitation (see Fig. 2). A subsequent study by Hansen et al. [15] confirmed that these excitations were caused by the depolarizing current of the SAC.

It is also believed that SAC play a role during mechanical impact to the chest, which may be either lethal or life saving. It is known that a sudden precordial impact of a small object into the chest can cause Commotio Cordis [16]: an arrhythmia which is lethal. Alternatively, a strong impact using the human fist on the chest during a cardiac arrhythmia (precordial thump), may terminate a cardiac arrhythmia. Both effects are believed to have a feedback on excitation mainly via stretch and SAC and are discussed in [16–21].

2. Modeling reaction-diffusion-mechanics

Modeling electrical activity. Electrical activity of the heart can be described by a system of reaction-diffusion (RD) equations and has been reviewed previously (see for example [5,22,23]). A standard monodomain model for cardiac tissue is given below.

$$\begin{aligned} C\frac{\partial V}{\partial t} &= \nabla\cdot(\mathbf{D}\nabla V) + I_m(V, g_i) \\ \frac{\mathrm{d}g_i}{\mathrm{d}t} &= \phi(g_i, V). \end{aligned} \tag{1}$$

The first equation describes changes of the transmembrane potential V on the cell membrane (with capacitance C) as a result of inward and outward transmembrane ionic currents I_m, and currents between adjacent cardiac cells $\nabla\cdot(\mathbf{D}\nabla V)$, where $\mathbf{D}$ is the conductivity tensor that accounts for the electrical anisotropy of cardiac tissue. For details and derivation of this equation see [5]. The ionic current I_m is a sum of all currents that flow across the cardiac membrane (see Fig. 1) (e.g. $I_m = I_{Na} + I_{Ca} + I_K + \cdots$). Each of these currents depend on other variables, which are called gating variables g_i and account for experimentally measured activation and inactivation kinetics of that specific current. There are many different types of models available for cardiac cells, which differ in complexity and details on the representation of ionic currents I_m. The first *biophysical* or ionic models were developed by Hodgkin–Huxley (for nerve cells) [24] and Noble (for cardiac cells) [25], and describe individual ion currents across the cell membrane based on detailed experimental observations. Modern ionic models in addition to ionic currents also describe concentration changes of the major ions involved. These models produce accurate properties of the cardiac action potential such as action potential shape, refractoriness, rate dependence, and describe the various detailed biophysical mechanisms of excitation that occur due to different dynamics of ion channels. These models often contain many ODEs (10–100) and can be computationally intensive. Ionic models can be used to study detailed quantitative effects of ion channels, e.g. drug applications, genetic disorders, etc. Some examples of these models are [26–28]. More simple *phenomenological* models describe basic macroscopic properties of cardiac tissue such as shape, refractoriness, etc. These models contain fewer ODEs (<4) and can be used to study more general qualitative effects. Some examples of these models are [29–32].

Modeling mechanical deformation. Cardiac cells change their length by up to 15% [33] during cardiac contraction. In order to model deformation, finite deformation elasticity theory should be applied to describe the kinematics of deformation and stress equilibrium and model the relationship between stress and strain.

Equations that describe finite deformation elasticity arise from the conservation of linear momentum following Newton's law of motion [34]. For static stress equilibrium in the absence of body forces, the governing equations expressed in terms of the second Piola–Kirchhoff stress components T^{MN} regarding mechanics are described by:

$$\frac{\partial}{\partial X_M}\left(T^{MN}\frac{\partial x_j}{\partial X_N}\right) = 0 \tag{2}$$

where, x_m is the deformed space, and X_m the undeformed space. The second Piola–Kirchhoff stress tensor describes material behavior independent of rigid body rotation and contains passive (T_p) and active stress (T_a) components described by:

$$T^{MN} = {T_p}^{MN}(\mathbf{E}) + {T_a}^{MN}(\mathbf{E}, V_a) \tag{3}$$

where, $\mathbf{E}$ is the Green-Lagrange deformation tensor, that accounts for mechanical deformation and V_a is a function that controls the

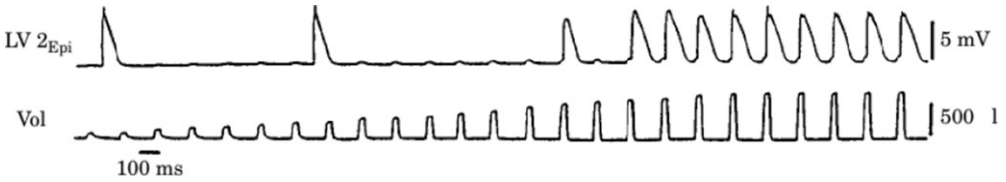

Fig. 2. Mechanically induced ectopic (abnormal) excitation in a Langendorff perfused rabbit heart (i.e. the aorta is cannulated and the heart is maintained by perfusion with an oxygen and nutrient rich solution). Monophasic action potential (MAP) (top) and changes in left ventricular volume (LVP) (bottom). Once a critical volume (i.e. stretch) is reached, an action potential is triggered. Published with permission from [14].

amplitude, delay and recovery of the active sress [35,36]. Passive properties are described by (non-linear) constitutive relations, which are determined by experimental models. Experimental evidence has shown that cardiac tissue exhibits different responses along various material axes [37], and this has important implications for both cardiac mechanics [38] and electrical activation in myocardial tissue [39]. Active properties (i.e., contraction) are related to the intracellular calcium concentration, which is typically one of the variables of the RD model (see Niederer et al. [40] for an extensive model description).

Modeling mechano-electrical feedback. Mechanical deformation affects the electrical properties in various ways: first, the coordinate system is changed during deformation thereby affecting diffusion properties; second, passive electrical properties such as capacitance and diffusion may change during deformation and third, ionic currents, such as SAC are affected by deformation. The effects of deformation (**E**) on the RD equation is schematically shown in Eq. (4):

$$C(\mathbf{E})\frac{\partial V}{\partial t} = \nabla \cdot (\mathbf{D}(\mathbf{E})\nabla V) + I(V, \mathbf{E}). \tag{4}$$

In [41,38,35,36] a modeling framework for MEF has been introduced. In Eq. (4) the system does not move. However, contraction of the coordinate system also affects the metric tensor of the coordinate system, which becomes curvilinear. Due to motion of the material coordinate system, we use a general curvilinear expression that is corrected for the deformation of the local area, to evaluate the Laplacian in Eq. (4). This is described in Eq. (5):

$$\nabla \cdot (\nabla \mathbf{V}) = \frac{\partial}{\partial X_M}\left(\sqrt{g} g^{-1}_{MN} \frac{\partial V}{\partial X_N}\right) \tag{5}$$

where, $g_{MN} = \{\frac{\partial x_k}{\partial X_M}\frac{\partial x_k}{\partial X_N}\}$ is the covariant metric tensor of the coordinate system, (which is directly related to the Green Lagrange deformation tensor **E** [34]); and g is the determinant of the metric tensor which accounts for local deformation.

The effect of contraction on the ionic current (SAC) has been investigated in several studies [42,43,18,36]. SAC have quite simple properties compared to other ionic channels. Their conductivity is time independent and only affected by stretch of the cardiac membrane and the experimentally measured current–voltage relationship for the SAC is almost linear (see Fig. 3a) [44]. Furthermore, the conductivity of the SAC is dependent on the cell's sarcomere length (SL) [44] and can also be approximated by a linear function (see Fig. 3b). This resulted in the following expression for SAC current, that was introduced in [42,43,18] and modified for strain dependency [36]:

$$I_{SAC} = G_{SAC}(\sqrt{g} - 1)(V - E_{SAC}) \tag{6}$$

where, G_{SAC} and E_{SAC} are the conductance and reversal potential for the SAC, respectively. Furthermore, it is widely believed that the current through the SAC occurs mainly during stretch and thus it is assumed that the current in Eq. (6) is only present if $\sqrt{g} > 1$. Adding Eq. (6) to the right hand side of Eq. (4) provides a description of the direct effect of stretch on the membrane current.

Numerical formulation. To solve the RDM model Nash and Panfilov [35] introduced a hybrid method in which an explicit Euler scheme was used for the RD system, with nonlinear finite element techniques for the large deformation mechanics. The solution procedure is described below.

After N time integration steps (a value of 3 was used in [36]) for solving the RD equations (Eq. (4)), the equations governing tissue mechanics are solved (Eqs. (2) and (3)), using active stress components produced by the variable V_a of the RD equations. Non-linear Newton iterations are performed to solve the stress equilibrium equations (Eq. (2)) and provide updated values of the Green-Lagrange deformation tensor, which modulate the excitation properties via Eqs. (4) and (6) for the subsequent N excitation time-steps. A detailed description of the solution procedure is given in [35,45].

Recently, a more extensive mathematical analysis involving numerical issues of soft tissue modeling on coupled electric-mechano systems was published in [46]. They showed in a more detailed numerical analysis that in some cases a more accurate integration scheme should be used to enforce stability of coupled reaction diffusion mechanics systems. This topic definitely requires more attention in the future for both stability issues and numerical efficiency.

3. Reaction-diffusion mechanics without SAC

One of the first studies regarding RDM were performed by Nash and Panfilov [35]. They used the Aliev–Panfilov model [31] to describe membrane kinetics for cardiac tissue. Material properties were given by Mooney–Rivlin material law [47] to describe mechanical isotropic material behavior. To couple the reaction-diffusion system with the mechanical part Nash and Panfilov [35] introduced an additional equation for active tension that described qualitatively consistent timing and amplitude of cardiac tissue contraction. The formulation did not include SAC nor the effects of mechanics on passive properties, and thus the only effects studied were the direct geometric effects of tissue deformation on wave propagation.

Nash and Panfilov investigated electromechanical activity following a point stimulus at the center of the tissue and compared this with the activity from a rotating spiral in the center of the tissue. They found that for the central location the overall mechanical deformation caused by a centrally located rotating spiral wave was an order of magnitude less than that of periodic radial waves, but deformations became comparable for non-central locations. They also studied the effects of MEF on spiral wave rotation. They found that spiral waves with MEF had a larger variation of periods compared to spiral wave periods in the non-contracting model and that the mean spiral wave period during contraction was slightly increased. They also found that in the absence of mechanical deformation spirals had a stationary circular meandering pattern, whereas with MEF spiral wave meandering was non-stationary and drifted along the boundary

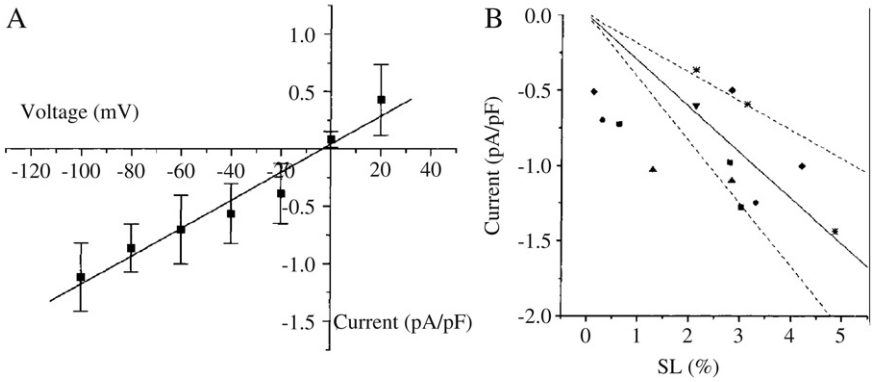

Fig. 3. (A) SAC current–voltage relationship normalized to cell capacitance [44]. (B) Linear regression of % change in SL vs. current density. Reprinted with permission from [44].

of the medium. The magnitude of these effects are small and no significant effect of MEF on spiral wave breakup was found. However, the effects of SAC on MEF was not investigated in that study.

4. Reaction-diffusion mechanics with SAC

In this section we review the effects of SAC on electrophysiological properties of cells and the effects of SAC on 1D and 2D wave propagation, which were studied using various modeling approaches and using various models of cardiac tissue.

The effects of SAC on electrophysiological properties. During stretch, SAC produce an inward current which tends to depolarize a cardiac cell and has various effects on electrophysiological properties. The effects of a constant, time independent current via SAC on general electrophysiological properties was studied by Trayanova et al. [43]. The model did not include active contraction and the effect of SAC was studied using only a RD model. With reference to Fig. 4, the paper [43] reports the following effects of SAC (for $G_{SAC} = 30\ \mu S/\mu F$ and $E_{SAC} = -20$ mV): (1) A slight decrease of resting membrane potentials (around −75 mV vs. −85 mV). (2) Elongation of the action potential for short cycle lengths (CL) (i.e., for a CL of 100 ms action potential duration is around 82 ms vs. 77 ms). (3) A slight flattening of the restitution curve. (4) A slight increase of the effective refractory period (up to 1–2 ms). (5) An increase of conduction velocity and wavelength for cycle lengths is longer than 115 ms, and a decrease for cycle lengths smaller than 115 ms. (6) An increase in the activation threshold. These findings reported by Trayanova et al. [43] are broadly consistent to those reported experimentally in [48–50].

Other studies [42,51] have shown that in extreme cases the current through SAC can prevent formation action potentials. This occurs as a result of the accommodation affect, in which the threshold of activation increases due to a slower depolarizing current [52,24]. This has also been reported in experiments [24]. Possible consequences of accommodation for wave propagation in cardiac tissue were studied by Biktashev et al. [53]. As we point out below, such blocks of propagation can cause breakup of spiral waves.

Studies have also investigated the effects of SAC on the action potential. Different responses are possible, which are determined by the timing of the stretch and the magnitude of I_{SAC} generated. If stretch is applied during the plateau (excitation) phase of the action potential, it will change the time course of repolarization, which leads to either shortening or lengthening of the action potential. This change in duration depends on the value of E_{SAC} and the magnitude of the transmembrane potential during the plateau phase; I_{SAC} can be either an outward or inward current. This also has been reported in both experimental [44,54] and modeling studies [43,19,55]. If SAC are activated when the cell is already repolarized, SAC may result in either a prolonged excitatory phase or a new action potential [43,36,55] (see Fig. 4).

Pacemakers. The idea of action potentials induced by SAC was further investigated in [36,45] where it was shown that in some conditions electrical waves can induce stretch of cardiac tissue, which in turn may be sufficient to initiate a new action potential resulting in the onset of periodical pacemaker activity. Panfilov et al. [36,45], used an Aliev–Panfilov [31] model to describe membrane kinetics, which was modified to describe SAC in accordance with Eq. (6). Fig. 5 shows wave propagation after application of a single stimulus at the center of a 2D medium, with and without mechanical activity. We see that without mechanics the initial wave vanished, while with mechanics a stable pacemaker sets up at the center of the medium. The mechanism of pacemaker activity here is simple and related to depolarization of tissue by the SAC. With reference to Fig. 5, we observed stretch at the center of the medium after the wave had traveled away from the center. This stretch resulted in an inward current via SAC and depolarized the resting tissue at the center, which resulted in the onset of subsequent periodic activations [36].

It was also shown that pacemaker activity occurred at locations pre-determined by the medium size, its electrical and mechanical properties and that the location of a pacemaker slowly drifts until it reaches a stationary position. Fig. 5 shows an comprehensive picture of pacemaker drift from different initial conditions to stable attractors for one set of parameter values. Further details on the effect of medium size on this process can be found in [36]. It was also shown in [45] that in a heterogeneous medium containing a gradient of excitability, pacemakers drift to the region with lower period values. Furthermore, mechanical deformation not only induces pacemakers but also has a pronounced effect on the spatial organization of excitation patterns (see Fig. 6) [45]. Paper [45] also reports on the interaction of multiple pacemakers. For example, for one parameter set multiple pacemakers were shown to drift toward each other and merge to form one stable pacemaker at the center of the tissue (see Fig. 6) [45].

Note that these studies were performed in simplified models of cardiac tissue and it remains to be determined whether these effects will be present using ionic models, as well as in experiments. Recently, it was shown in neonatal rat ventricular cell cultures that calcium overload can lead to pacemaker activity and that in some cases pacemakers drift throughout the medium [56]. Mechanisms of this drift require further investigations.

Drift of spirals. In the previous section, we discussed drift of spiral waves due to mechanical deformation in the absence of SAC [35]. A more recent article [51] studied the effects of mechanical deformation and SAC on spiral wave behavior. For this study, a different RD model was used: a modified version of the three

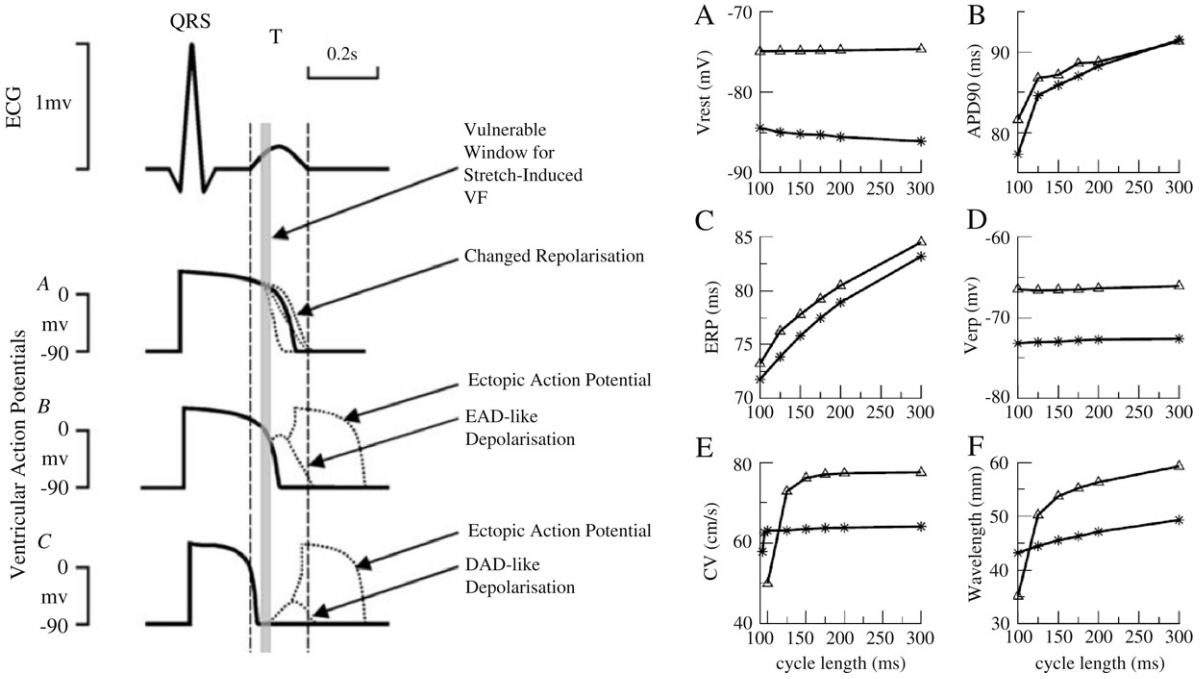

Fig. 4. Left: Effects of mechanical impact action on mechano-sensitive channels on AP shape during a critical time window. Reprinted with permission from [17]. Right: Basic electrophysiological properties with (triangles) and without SAC (stars). (A) Resting membrane potential. (B) Action potential duration at the level of 90% repolarization (APD_{90}). (C) Effective refractory period (ERP). (D) Transmembrane potential at the end of ERP. (E) Conduction velocity (CV). (F) Wavelength (ERP × CV). Reprinted with permission from [43].

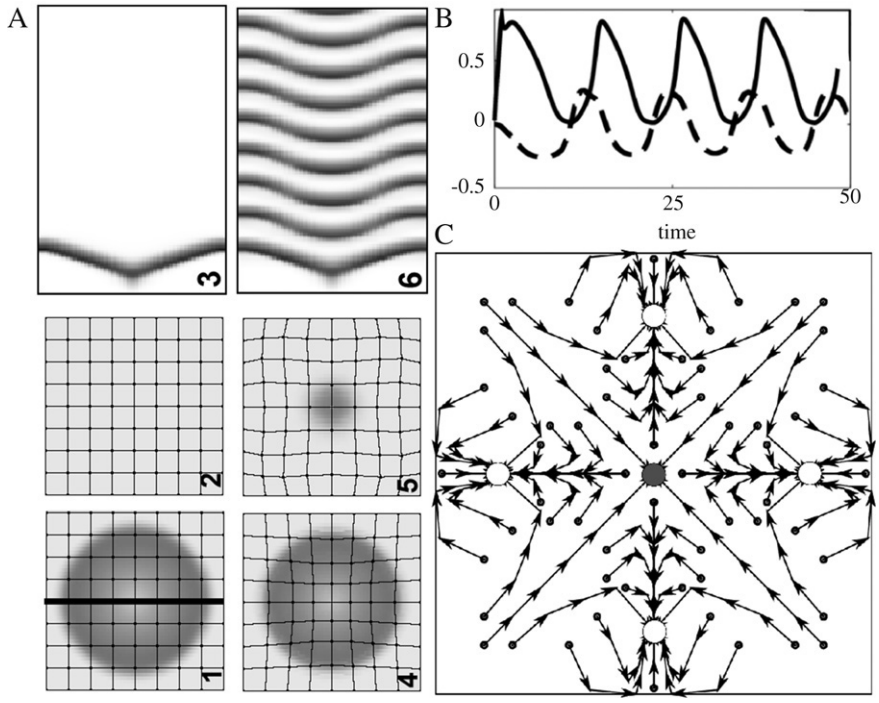

Fig. 5. (A) Development of pacemaker activity due to mechanics. (B) Time course of the excitation variable (solid line) and dilatation ($\sqrt{g} - 1$) (dashed line). (C) Drift of pacemakers from different initial conditions. Reprinted with permission from [36].

variable Fenton–Karma model [32], which contains a more detailed description of the sodium current in comparison to the previous used Aliev–Panfilov model. In this model, SAC were modeled using Eq. (6). Panfilov et al. [51] showed that in the presence of mechanical deformation, the spiral wave drifted to the center of the medium, which was an attractor of this system independent of the initial starting position (see Fig. 7A). After arriving at the attractor, the tip of the spiral wave underwent a bi-periodic hypo-cycloidal motion. The drift was primarily due to the SAC. When SAC were removed from the model (i.e. the model had only geometrical feedback as in [35]), the spiral wave drift was still present, but the tip was no longer directed to the stable attractor in the center of the tissue. Instead, it drifted along the boundary. Drift velocity was also much smaller. When I_{SAC} alone was used (i.e., no geometrical feedback), drift and meander to the center of the medium were observed in a way similar to Fig. 7A. It was also shown that different

Fig. 6. Top: Drift of a single pacemaker. Bottom: Interaction and drift of multiple pacemakers. Reprinted with permission from [45].

medium sizes did not affect the position of the stable attractor, but did affect the drift velocity.

As suggested in [51], spiral wave drift is induced by a periodic modulation of the properties of the medium due to contraction. This mechanism is similar to the resonant drift mechanism of spiral waves and has been studied in [57,58]. In particular, it was shown in [57,58] that if the properties of the excitable medium are changed periodically, this results in the onset of spiral wave meander. If this period is close to the period of the spiral wave, then spiral wave drift is observed. In our case, contraction induced by a rotating spiral provides such a periodical modulation with a period equal to that of the spiral wave. Thus spiral wave drift is expected. Resonant drift of spirals have been observed in detailed ionic models of cardiac tissue [59,60] and in BZ experiments [58].

Breakup of spirals. The study of Nash and Panfilov [35] did not report any effects of mechanical deformation on spiral wave breakup. However, the subsequent study of Panfilov et al. [51], which included SAC and a different description of the RD model, reported that mechanical deformation can induce breakup of spiral waves. Fig. 7B shows a typical pattern of mechanically induced breakup using a three variable Fenton–Karma model [32]. Here, we see that after a few rotations, the initial spiral wave blocked at certain positions, which caused the spiral to breakup into fragmented spirals. Mechanically induced spiral breakup was due to the SAC. When SAC were removed (i.e., leaving just the geometry feedback), the spiral remained stable and did not break up. On the other hand, when only I_{SAC} was used (with no geometrical feedback), the spiral wave broke-up.

Spiral wave fragmentation was shown to occur due the accommodation effect of the SAC. The sodium current is the main determinant in the generation of a new action potential, and its magnitude is proportional to the product of the sodium activation and inactivation gates, which are time and voltage dependent. If at any time there is a voltage difference between two neighboring cells (e.g., if one cell is excited and the other cell remains in its resting state), then ion current flows from one cell to the other via the gap junctions and slowly raises the membrane potential. When the threshold value (approximately −60 mV) is reached, the inward sodium current is activated and a new action potential is generated, which in turn activates the next neighboring cell. However, due to the accommodation effect, SAC have already *slowly* depolarized the tissue (before any neighboring cell is excited) thereby effecting the inactivation kinetics of the sodium channel. Thus, when a fully excited neighboring cell tries to depolarize this cell via the gap junctions (which is a faster process compared to the SAC), the sodium current cannot be activated, because the inactivation gates are already closed due to the slow rising potential of the SAC. This is shown in Fig. 7C by the black arrow. A similar mechanism was reported in [61] for a 1D setup using a more accurate ionic model of cardiac tissue (Courtemanche model [27]). Inactivation of the sodium current has also been observed in experiments [24].

Fig. 7. Spiral drift and breakup caused by mechanical activity. See text for explanation. (A) Drift of spirals from different initial conditions. (B) Spiral wave breakup due to accommodation effect. (C) Time course of the excitation variable and the sodium current measured in the black square of Figure B. The black arrow denotes the point in which the SAC blocks the sodium current. Modified from [51].

Inducing spiral waves by mechanical stimulation (Commotio Cordis). Induction of spiral waves by mechanical stimulation has been studied in order to understand possible mechanisms of the initiation of ventricular arrhythmias after a mechanical impact (Commotio Cordis). Using 2D modeling, Garny and Kohl [19] investigated the effects of mechanical impact on the initiation of spiral waves. They used a guinea pig ventricular cell model [62] for the RD model. They added SAC to represent a bell shaped profile of external forces and thus to simulate a region of impact, within which mechanically induced changes to the electrophysiology occurred via the SAC. SAC were described using $I_{SAC} = G_{SAC}(V - E_{SAC})$ and this current was activated during impact (for details see [19]). They found that various responses can occur, depending on the timing of the impact during the action potential. Garny and Kohl showed that if the mechanical impact was applied between 10% and 50% repolarization of the action potential (i.e., which is similar to the vulnerable window in the left panel of Fig. 4), this can lead to the initiation of self sustaining spiral waves. This is shown in Fig. 8. The SAC depolarize the tissue behind the action potential, and a new action potential arises that propagates in some directions, but is blocked in other directions (see Fig. 8 at 17 and 31 ms). As a result two spirals are born. Garny and Kohl showed that there is only a very narrow time window for which such spiral waves can be initiated [19,55]. This has also been observed in experiments by Link et al. [16].

Similar results have been reported by Li et al. [18], who investigated the induction of ventricular arrhythmias after a